



HAL
open science

Spin Density Distribution in Open-Shell Transition Metal Systems: A Comparative Post-Hartree–Fock, Density Functional Theory, and Quantum Monte Carlo Study of the CuCl₂ Molecule

Michel Caffarel, Emmanuel Giner, Anthony Scemama, Alejandro Ramírez-Solís

► To cite this version:

Michel Caffarel, Emmanuel Giner, Anthony Scemama, Alejandro Ramírez-Solís. Spin Density Distribution in Open-Shell Transition Metal Systems: A Comparative Post-Hartree–Fock, Density Functional Theory, and Quantum Monte Carlo Study of the CuCl₂ Molecule. *Journal of Chemical Theory and Computation*, 2014, 10 (12), pp.5286-5296. 10.1021/ct5004252 . hal-01121580

HAL Id: hal-01121580

<https://hal.science/hal-01121580>

Submitted on 29 Jan 2020

HAL is a multi-disciplinary open access archive for the deposit and dissemination of scientific research documents, whether they are published or not. The documents may come from teaching and research institutions in France or abroad, or from public or private research centers.

L'archive ouverte pluridisciplinaire **HAL**, est destinée au dépôt et à la diffusion de documents scientifiques de niveau recherche, publiés ou non, émanant des établissements d'enseignement et de recherche français ou étrangers, des laboratoires publics ou privés.

Spin density distribution in open-shell transition metal systems: A comparative post-Hartree-Fock, Density Functional Theory and quantum Monte Carlo study of the CuCl_2 molecule

Michel Caffarel, Emmanuel Giner, Anthony Scemama, and Alejandro Ramírez-Solís*
CNRS-Laboratoire de Chimie et Physique Quantiques, IRSAMC. Université Paul Sabatier,
118 route de Narbonne, 31062 Toulouse Cedex, France

We present a comparative study of the spatial distribution of the spin density (SD) of the ground state of CuCl_2 using Density Functional Theory (DFT), quantum Monte Carlo (QMC), and post-Hartree-Fock wavefunction theory (WFT). A number of studies have shown that an accurate description of the electronic structure of the lowest-lying states of this molecule is particularly challenging due to the interplay between the strong dynamical correlation effects in the $3d$ shell of the copper atom and the delocalization of the $3d$ hole over the chlorine atoms. It is shown here that *qualitatively* different results for SD are obtained from these various quantum-chemical approaches. At the DFT level, the spin density distribution is directly related to the amount of Hartree-Fock exchange introduced in hybrid functionals and, therefore, it is not possible to draw conclusive results. At the QMC level, Fixed-node Diffusion Monte Carlo (FN-DMC) results for SD are strongly dependent on the nodal structure of the trial wavefunction employed. In the case of this open-shell system, the $3N$ -dimensional nodes are mainly determined by the 3-dimensional nodes of the singly occupied molecular orbital (SOMO) and FN-DMC results are found to be strongly dependent on the type of one-particle model used for generating the SOMO (here, Hartree-Fock or Kohn-Sham with a particular amount of HF exchange). Regarding wavefunction approaches, HF and CASSCF lead to strongly localized spin density on the copper atom, in sharp contrast with DFT. To get a more reliable description and shed some light on the connections between the various theoretical descriptions, Full CI-type (FCI) calculations are performed. To make them feasible for this case a perturbatively selected CI approach generating multi-determinantal expansions of reasonable size and a small tractable basis set are employed. Although semi-quantitative, these near-FCI calculations allow to clarify how the spin density distribution evolves upon inclusion of dynamic correlation effects. A plausible scenario about the nature of the SD is proposed.

I. INTRODUCTION

In spite of much effort in the last 50 years, to devise a general electronic structure approach that is both computationally practical and accurate enough for all types of molecular systems is still a challenging task. Indeed, to provide a truly accurate account of the electronic structure of a molecule one must take into account in a *balanced* way several effects of different physical/chemical nature, a) electron-electron correlation effects (resulting from the $1/r_{12}$ interaction), b) exchange effects (Pauli principle), c) delocalization (kinetic effects) and, in some cases, d) quasi-degeneracy effects (quantum entanglement of almost degenerate low-energy wavefunction components). All the present-day methods deal with these aspects in different ways, sometimes with not so-clear distinctions between them (*e.g.* the mixture of exchange and non-dynamical correlation effects within Kohn-Sham formulation of Density Functional theory). Here, in our study we shall consider the two most widely used electronic structure methods, namely Density Functional Theory (DFT) and molecular orbital-based or wavefunction theories (WFT) (post-Hartree-

Fock approaches). We shall also consider quantum Monte Carlo (QMC) methods that are potentially very accurate but are still methods of confidential use in quantum chemistry due to a number of practical/theoretical limitations. Each type of method treats the various effects cited above in different ways with particular strengths and weaknesses.

Density functional theory (DFT) is nowadays the most popular and widely used theory for the description of electronic structure of atoms, molecules and condensed phases (solids and liquids). Its success stems mainly from the fact that it provides reasonable energetic and structural properties at a moderate computational cost. One of the most fundamental tenets of DFT is that it expresses the general N -body interacting electronic system into a much more simple effective one-body system where electrons are immersed into a universal exchange-correlation potential embodying all the complexity of the N -body problem. Within this formalism all types of electronic systems, regardless of the strength and characteristic length of the interactions involved (*i.e.* covalent, ionic, hydrogen-bonded, metallic or van der Waals types) are expected to be treatable, at least in principle. However, many questions remain open in the DFT realm, mostly due to the necessity of approximating in a coherent way the unknown universal exact exchange-correlation functional. In the last 20 years DFT has made very important progress, mainly due to the improvements over Gener-

*On sabbatical leave from Facultad de Ciencias, Universidad Autónoma del Estado de Morelos, México

alized Gradient Approximation (GGA-type) functionals: The meta-GGA functionals[1–3] which use the kinetic energy densities ($\tau_{\uparrow}, \tau_{\downarrow}$) and/or the Laplacian of the density as non-local variables, and hybrid adiabatic connection functionals[4] that empirically mix Hartree-Fock (HF) non-local exchange with GGA exchange. However, all the hybrid functionals contain several adjustable semi-empiric parameters. Some of the hybrid functionals have become extremely popular since they yield, in general, rather good energetic and structural results for main-element molecules. Nevertheless, fundamental problems still appear, for example the fact that many of these semi-empirically adjusted exchange-correlation (xc) functionals do not even provide the correct asymptotic exchange-correlation potential for systems for which the exact behavior is known.[5]

In the case of WFT the quantum chemical description passes through the construction of an explicit wavefunction with the need of accurately introducing static and dynamic electronic correlation effects. Ideally this can be achieved through the construction of the Full Configuration Interaction (FCI) wavefunction. However, since for most molecules the FCI solution is readily out of reach even with moderate basis sets (exponential increase of the Hilbert space), approximate solutions are needed and are achieved in practice by building increasingly complex wavefunctions following one of several approximations using either perturbation, truncated CI (CIS, CISD, CISDQ, CISDTQ,...) or coupled cluster (CCSD, CCSD(T), ..) techniques. Note that, within the WFT framework, the question of whether or not the electronic state in question can be correctly described using single-reference methods also appears. In the negative case the application of the Complete Active Space SCF (CASSCF) method has become customary and the ensuing CASSCF wavefunction is used as zeroth-order reference for further treatment of the dynamic correlation effects, for instance, through the CASPT2 or the Averaged Coupled Pair Functional (ACPF) methods. At this point we emphasize that for the spectroscopic properties of transition metal molecules such as the CuCl_2 molecule treated here, critical accuracy problems might arise due to the quality of the atomic basis sets used or to the quality of the electronic correlation treatment. Unfortunately, the application of very accurate wavefunction methods is still restricted to molecules with a few atoms due to the rapid growth of the computational cost with the number of electrons (or the number of atomic basis functions).

The third type of methods considered here are the so-called quantum Monte Carlo (QMC) approaches. QMC are statistical methods for solving the Schrödinger equation. They are very attractive since they are potentially exact methods (up to the statistical errors inherent to any Monte Carlo approach). Unfortunately, in practice we have to cope with the pathological fluctuations of the wavefunction sign and a so-called fixed-node approximation has been introduced to fix this prob-

lem. This approximation can be viewed as solving the electronic Schrödinger equation but with a new additional constraint, namely, imposing the solution to vanish wherever a known trial wavefunction given as input vanishes. In other words, the nodal hypersurface of the fixed-node wavefunction (nodes= $3N$ -dimensional hypersurface where the wavefunction vanishes) are imposed to be identical to those of the approximate trial wavefunction. Numerical experience has shown that the fixed-node error is small according to the quantum chemistry standards (typically, a small percentage of the correlation energy for total energies) but, unfortunately, still large enough to lead to potential difficulties when computing the small energy differences involved in quantitative chemistry. Stated differently, suitable cancellation of fixed-node errors are needed. At this point, it is worth emphasizing that the need of suitable cancellation of errors in energy differences is of course not restricted to QMC and is, unfortunately, one of the most critical issues common to all computational chemistry approaches developed so far. In practice, it has been observed that the nodal quality is directly related to the physical/chemical content of the trial wavefunction. In short, the better the trial wavefunction is, the smaller the fixed-node error is. Let us emphasize that the need of having a rather good trial wavefunction to start a QMC calculation brings back some heuristics into the approach, a crucial point one has to be aware of. This aspect will be exemplified in the case of the CuCl_2 molecule treated in this work.

As seen, for different reasons none of these state-of-the-art approaches are fully satisfactory to deal with all types of molecular problems. Here, we propose to shed some light on their theoretical and practical relationships on a small molecule which is representative of a difficult molecular problem, namely, the ground state properties of the CuCl_2 molecule. As shown in previous studies, even the determination of the nature of the ground state and the proper energetic ordering of the low-lying states of this molecule turns out to be particularly difficult. This is mainly due to a subtle interplay between the delocalization of the $\text{Cu}(3d)$ hole on the molecular axis and the dynamic correlation effects. Here, in order to investigate such relationships we focus on the spatial distribution of the spin-density of the ground-state along the molecular axis, which is the main physical quantity associated to the relative stability of the lowest electronic states in CuCl_2 . More precisely, we consider the difference of α and β spin densities integrated within the plane perpendicular to the molecular axis (actually, a parallelepiped of small thickness). Our working definition is

$$\Delta\rho(z) = \int_{z-\epsilon/2}^{z+\epsilon/2} dz \int \int dx dy [\rho_{\alpha}(\mathbf{r}) - \rho_{\beta}(\mathbf{r})], \quad (1)$$

where z is the coordinate along the molecular axis of the linear centro-symmetric molecule, the copper atom being at the origin, and ϵ is a small positive parameter (here, chosen equal to 0.1 a.u.) corresponding to the

thickness of the parallelepiped. For simplicity this partially integrated difference of α and β densities will be shortly referred to in the present work as the spin density (SD) distribution. Although the DFT approaches lead to a slightly different optimized geometry (*ca.* 3.92-3.97 a.u.), in what follows we shall use the equilibrium centro-symmetric geometry fixed at a Cu-Cl distance of 3.9 a.u., closer to the experimental value of 3.85 a.u. for the ground state.

The contents of the paper are as follows. In Sec. II we summarize what is known about the nature of the low-lying electronic states of CuCl_2 . Sections III,IV,V, and VI present the results obtained for the spatial distribution of the spin density using DFT, WFT, QMC and near-Full CI, respectively. Finally, in Sec. VII a detailed summary and discussion of the results obtained is presented. In particular, a plausible description of the nature of the ground state is proposed.

II. WHAT IS KNOWN ABOUT CuCl_2

The quantitative description of the electronic structure of metal-containing systems is known to be a rather delicate problem. Regarding DFT studies, we can mention three articles reporting extensive tests of a series of functionals on transition metal (TM) containing molecules. Schultz *et al.*[6] propose a data set of bond lengths for 8 selected TM dimers, their atomization energies and use these for testing DFT, while Furche and Perdew[7] also investigate the performance of contemporary semi-local (GGA, meta) and hybrid density functionals for bond energetics and structures of 3d transition-metal compounds. In this direction, one of us reported[8] a systematic study on the performance of local, semi-local and non-local xc functionals for the lowest singlet-triplet transition in AgI, showing that a rather unpredictable and thus, unreliable, performance of the various types of functionals appears for this singlet-triplet transition. Although the CuCl_2 molecule was not included in these studies, its spectroscopy presents a particularly difficult case for *ab initio* and DFT methods, since important correlation effects (arising mainly in the 3d shell of copper) are strongly coupled to charge transfer effects via the 3p orbitals of the Cl ligands. Fortunately, the low-lying transitions are experimentally quite well known[9, 10] and two extensive benchmark variational multireference Averaged Coupled Pair Functional(CASSCF+ACPF) studies on the spectroscopy of CuCl_2 exist; there the attention was focused on the nature of the three lowest electronic states[11, 12] that give rise to the four observed transitions. The first three ligand field (LF) states are thought to arise from d-d transitions on the copper ion and they can be described by a different orientation (σ , π or δ) of the singly occupied HOMO, in principle, the localized Cu(3d) hole. So, at this point one might ask why is this such a complicated problem? In order to understand the complexity

in the spectroscopic description involving the five lowest ligand-field (LF) and charge-transfer (CT) states note that, at the doubly ionic limit, CuCl_2 is described by the $\text{Cl}^- \text{Cu}^{2+}(3d^9) \text{Cl}^-$ structure, while in the covalent ClCuCl description, the copper atom which is promoted to the $3d^9 4s^2$ excited state undergoes 4s-4p hybridization and can establish covalent bonds with both Cl atoms. An intermediate situation arises when one considers the resonant $\text{Cl}^- \text{Cu}^+(3d^9 4s^1) \text{Cl}$ and $\text{ClCu}^+(3d^9 4s^1) \text{Cl}^-$ ionic structures. Near the equilibrium geometry, the exact electronic structure for all states is a mixture of these three valence situations. The first three LF states (${}^2\Sigma_g^+$, ${}^2\Pi_g$, ${}^2\Delta_g$) correspond to d-d transitions on the copper ion and it is generally thought that they can be described by the σ , π or δ orientations of the singly occupied Cu(3d) orbital. It is known that a correct description of electronic structures, and even more with such close lying states, must include a correct description of correlation effects especially important for the d shell, but also must allow for large repolarization differential effects between localized d-d states and charge transfer states. We stress that single-reference methods like Coupled Pair Functional(CPF) and CCSD(T) can be used here, since the HF wavefunctions are excellent zeroth-order approximations for the lowest electronic states of CuCl_2 [13]. From the DFT perspective, this feature is also very convenient, since standard Kohn-Sham based methods are, in principle, well adapted to describe transitions where only a change in the orientation of the 3d-hole in the central metal atom is involved. We stress that the ${}^2\Pi_g \rightarrow {}^2\Sigma_g^+$ transition in CuCl_2 represents a most difficult problem from the quantum theoretical point of view, since it has been predicted to range from -2495 to 6930 cm^{-1} . [14]

On the other hand, since the lowest five electronic states (all doublets) of CuCl_2 belong to different spatial symmetries, it has been possible to study these states through the Δ SCF approach in the DFT framework[14-16]. In this approximation each state, which is the ground state for a given spin and space symmetry, is optimized independently. Therefore, the main goal of[14] was to perform a coherent assessment of DFT results with benchmark *ab initio* calculations, eliminating the discrepancies found in previous studies so that the comparison was restricted to the basic ideas of DFT. The DFT calculations were done with the same relativistic effective core potentials (RECPs) and optimized extended basis sets used in Refs.[11] and [12]. Table I presents some selected DFT (LDA,GGA, hybrid and meta) and the *ab initio* ${}^2\Pi_g \rightarrow {}^2\Sigma_g^+$ transition energies along with the corresponding spin densities on the central Cu atom. Note that, within the *ab initio* framework, the dynamic correlation effects that control the nature of the Cu 3d-hole in the ground state are extremely difficult to obtain correctly since the SCF, the SDCl, and even the usually very accurate SDCl+Q (with Davidson's approximate size-consistent correction) schemes, all wrongly lead to a ${}^2\Sigma_g^+$ ground state. Only more sophisticated size-consistent *ab initio* methods like the Coupled Pair Func-

Method	${}^2\Pi_g \rightarrow {}^2\Sigma_g^+$	${}^2\Pi_g$ SD	${}^2\Sigma_g^+$ SD
LDA(S+VWN5)	6539	0.316	
BLYP	4802	0.429	1.04
PBE96	4699	0.43	1.03
HCTH407	4345	0.420	
OPTX-LYP	3963		
TPSS	4065	0.406	
M06-2X	3251	0.648	
B3LYP	1703	0.57	1.07
B97-2	1465	0.54	1.03
PBE0	756	0.64	1.08
NR-SCF ^a	-2495	0.962	
CASSCF(21,14)	6930	0.94	1.00
CASSCF+ACPF	232		
CASPT2	3861		
NR-SDCI ^a	-2116		
NR-SDCI+Q ^a	-1856		
CCSD(T)	859		
NR-Coupled Pair Functional ^a	659		
Theor. ^b	900		
Exp. ^c	253, 303, 475		

TABLE I: DFT, *ab initio* and experimental transition energies in wavenumbers, Mulliken spin densities (SD) on the Cu atom where available.

^a Non-relativistic calculations from [13].

^b Theoretical spin-orbit deconvoluted value from [11].

^c Experimental fine-structure transition energies; see corresponding references in [14].

tional (CPF), CCSD(T) or CASSCF+ACPF are able to correctly predict a ${}^2\Pi_g$ ground state, lying 659, 859 and 232 cm^{-1} (respectively) below the ${}^2\Sigma_g^+$ one without spin-orbit (SO) effects. Note that, at the purely electronic level, transition energies must be compared with the theoretical SO-deperturbed value, estimated to be 900 cm^{-1} . [11] We also stress that Bauschlicher and Roos[13] showed that the Darwin and mass-velocity relativistic effects cancel out nicely for the spectroscopy of this molecule and, for this reason, they were able to use all-electron non-relativistic (NR) calculations; in what follows we shall also make use of this fact. From the DFT perspective, most functionals (GGA, hybrid and even meta-ones) like HCTH407, BLYP, PBE96, OptX-LYP, TPSS and M06-2X largely overestimate this transition, all yielding values above 3200 cm^{-1} . Note that up to date, it is impossible to decide *a priori* which functional is to be used and which one can be trusted to yield reliable transition energies for an arbitrary metallic molecule. The delicate issue of the parametrization of most exchange-correlation functionals without the inclusion of transition metal containing systems has been discussed[14] in this context. It is somewhat ironic that much less expensive and sophisticated descriptions such

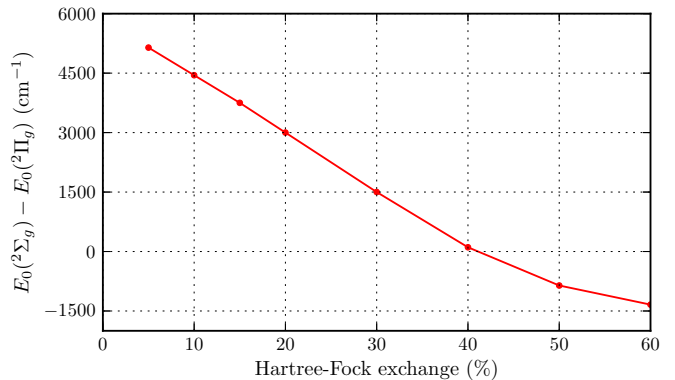


FIG. 1: ${}^2\Pi_g \rightarrow {}^2\Sigma_g^+$ transition energy (wavenumbers) with B3LYP as a function of the HF exchange percentage employed; positive values correspond to a ${}^2\Pi_g$ ground state, in agreement with experiment.

as those given by the PBE0 (750 cm^{-1}) and the B97-2 (1400 cm^{-1}) functionals yield better approximations to this transition energy than the very computational demanding benchmark CASSCF+ACPF one at 232 cm^{-1} . So the natural question arises: Are these hybrid PBE0 and B97-2 densities correctly describing each electronic state, therefore providing truly accurate total energies, or is this energy difference hiding some cancellation of errors associated with physically relevant quantities, such as the spatial distribution of charge and spin densities?

Although the various results presented in Table I may appear rather diverse, a clear trend can be perceived in the DFT subset, namely the role of the amount of HF exchange in the relative stability of both states. The larger the percentage of HF exchange in the functional the more stable the ${}^2\Sigma_g^+$ state becomes. In the extreme case of SCF-HF, we find the largest (negative) transition energy with ${}^2\Sigma_g^+$ state as the ground-state. In the opposite case where no HF exchange is included (BLYP, for instance), the ${}^2\Pi_g^+$ state becomes the ground state with a large (positive) transition energy. In between, one can see that for functionals having a fraction of HF exchange, this transition energy is still positive but smaller. To illustrate quantitatively this idea we present in Figure 1, for the B3LYP functional with variable HF exchange, the evolution of the transition energy *vs.* the HF exchange percentage.

This figure illustrates in a particularly striking way the high level of arbitrariness present when using hybrid functionals, such as B3LYP, for this system. Clearly, there is no rational way to decide which is the “right” amount of HF non-local exchange to be used.

Another quantity related to this aspect (via the localization of the 3d hole) is the spin-density on the central copper atom. In Table I, we present the values of several LDA, GGA and hybrid DFT-derived Mulliken spin-densities (SD) on the central Cu atom and the *ab initio* CASSCF values for both states, each at its equilibrium geometry. Note that both CASSCF wavefunctions were

optimized considering 21 active electrons (11 from Cu and 5 from each Cl atom) in 14 active orbitals, leading to large expansions with about 23 000 CSF. Clearly, a rather different picture of the spin-density distribution is obtained with the DFT-derived methods *vs.* the corresponding *ab initio* ones, especially for the ${}^2\Pi_g$ state. It is quite remarkable that the quality of the excitation spectrum obtained with these functionals can be related to the magnitude of the spin-density on the central metal atom, since although all the functionals yield $SD(\text{Cu})$ values close to 1.0 for the ${}^2\Sigma_g^+$ state, the corresponding value for the ${}^2\Pi_g$ ground state shows large variations between the good and bad-performing functionals. The PBE0 $SD(\text{Cu})$ value is 0.64, while the BLYP and PBE96 spin-densities on copper are only 0.43. An intermediate situation arises for the next two best performing functionals, B3LYP and B97-2, with larger values of 0.57 and 0.54. The CASSCF(21,14) spin-densities are both very close to 1 for both electronic states, and this is precisely why it is generally thought that these ligand states actually present a much more localized hole on the central copper atom than any of the DFT descriptions provide. We shall address this important point in more detail in what follows.

III. GROUND-STATE SPIN DENSITY WITH DFT

Having in mind the previous results, we start our analysis of the ground state spin density along the molecular axis with the DFT approaches. Note that the essential of chemical/physical properties of the molecule takes place via the singly-occupied molecular orbital (SOMO). It is so since in the spin-restricted Kohn-Sham formalism the contribution to the spin density resulting from all lower-lying orbitals cancels out and the local spin density is directly written as the square of the singly occupied orbital (other orbitals also contribute but in an indirect way through the Kohn-Sham optimization). The σ or π symmetry of the SOMO defines the overall symmetry of the ground state. In Figure 2 the SOMO orbital obtained with B3LYP for the ${}^2\Pi_g$ ground state as a function of the internuclear axis z for different values of HF exchange percentage are shown, along with the ROHF orbital (100% of HF exchange). The basis set used is that optimized in a previous work.[11] Since these orbitals are centro-antisymmetric with respect to the central Cu atom, only the $z > 0$ -region is shown. In this figure, the y coordinate is fixed to zero and x to 0.15, a value close to the maximum of the highest peak of the orbital. Recall that in the present case of a one-determinant restricted KS or HF representation, the spin density as defined in Eq.1 reduces to the integrated value over (x, y) of the square of this latter orbital. Figure 3 gives the B3LYP spin-densities obtained as a function of the HF exchange percentage together with the HF spin density. The two-peak structure of the SOMO (Figure 2) and SD

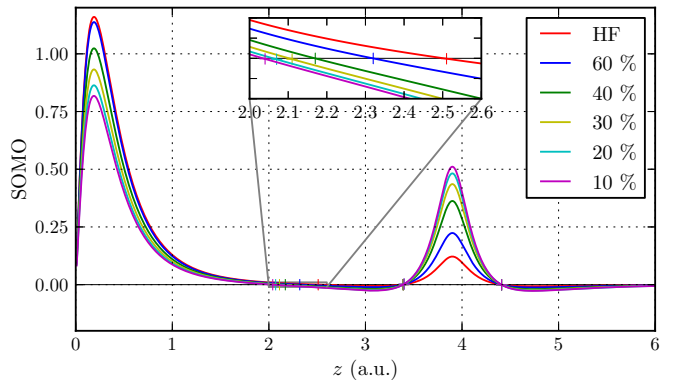


FIG. 2: Plot of the singly occupied molecular orbital along the nuclear axis $z > 0$ (copper at origin and chlorine at $z=3.9$ a.u.) for the ${}^2\Pi_g$ ground-state using B3LYP as a function of the HF exchange percentage used in the hybrid functional. The values of x and y are fixed to 0. and 0.15, respectively. The inset is a blow-up of the region in the middle of the bond where the SOMO vanishes. See discussion in Sec.V.

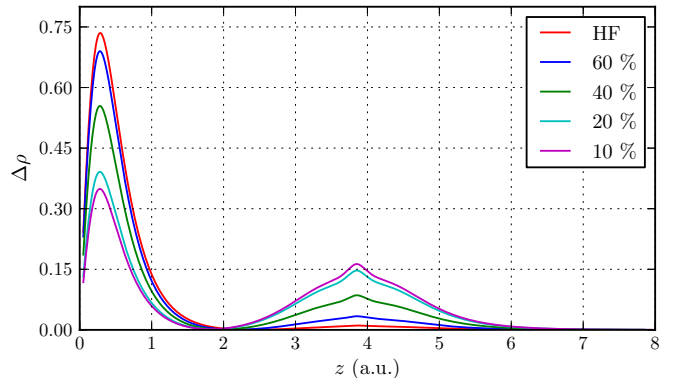


FIG. 3: Ground-state spin density with B3LYP as a function of the HF exchange percentage. Cu at the origin and Cl atoms located at $z=\pm 3.9$ a.u.; only the positive z axis is shown

(Figure 3) is clearly seen, one peak localized very close to the central Cu atom and the other on the chlorine atom. The relative height between the two maxima is strongly dependent on the percentage of HF exchange considered. In the case of HF (100% of HF exchange) the main peak is the highest one while the secondary peak on Cl is 20 times smaller. This indicates a highly localized character for the 3d hole at the HF level. When decreasing the percentage of HF exchange in B3LYP, the level of localization is found to decrease uniformly. Note also that the location of the zero (node) of the SOMO in the middle of the bond (see blow-up in Figure 2) is very dependent on the level of HF exchange. This result will be discussed in the context of the FN-DMC results (see Sec.V). As in the case of the ${}^2\Sigma_g^+ \rightarrow {}^2\Pi_g$ transition energy presented above, there is no physically meaningful reason to decide which amount of non-local HF exchange should be used in B3LYP for this metallic system.

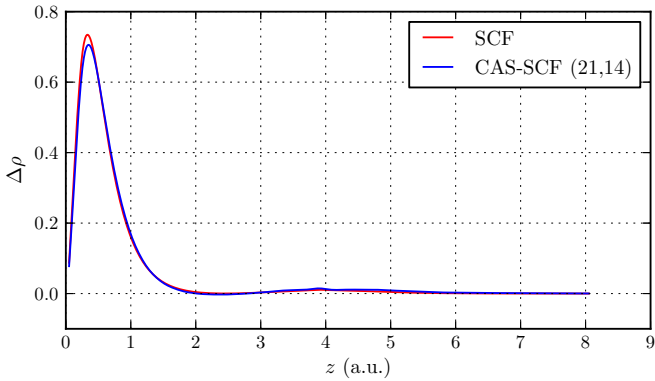


FIG. 4: ${}^2\Pi_g$ state spin density along the molecular axis (in a.u.) at the HF-SCF and CASSCF levels.

IV. GROUND-STATE SPIN DENSITY WITH WFT: HF AND BEYOND

Let us now turn our attention to the spin densities obtained from wavefunction approaches (WFT) at different levels of theory. Figure 4 shows $\Delta\rho(z)$ obtained for the ${}^2\Pi_g$ ground-state using both ROHF and CASSCF calculations. In the later case the active space chosen includes 14 orbitals (3s and 3p shells of both Cl, 4s and 3d shells for Cu) and 21 valence electrons (5 from each Cl and 11 from Cu) are distributed among them. In the resulting CASSCF(21,14) expansion the HF coefficient is found to be rather large (0.95), thus indicating a strong single-reference character of the ground-state wavefunction. Therefore, dynamic correlation effects largely dominate this problem. Note that the CASSCF spin-density distribution presented has been obtained by considering only the first one hundred determinants corresponding to the largest coefficients in the expansion. As seen in Figure 4 and expected from the single-reference nature of the wavefunction, HF and CASSCF spin-densities are almost identical. In both cases the 3d hole is found to be strongly localized on the copper atom and almost no SD is present on the chlorine atoms. As shown in Table I, only the use of highly correlated methods (CCSD(T), CPF or ACPF) can recover the correct energetic ordering of the two lowest electronic states. Unfortunately, given the huge number of CSF (ca. 7×10^9) considered in these approaches, the spin density distributions at these levels of theory are not available.

V. GROUND-STATE SPIN DENSITY WITH QUANTUM MONTE CARLO

In this section we report all-electron quantum Monte Carlo (QMC) calculations of spin-densities. Several versions of QMC have been introduced in the literature; however, they all rely on the very same ideas and differ only by technicalities. Here we employ a variant of the Fixed-Node Diffusion Monte Carlo (FN-DMC) method

defined with a constant number of walkers. For details the interested reader is referred to the original work.[17] In FN-DMC we are faced with two main sources of error: the statistical error inherent to any Monte Carlo approach and the fixed-node error. Other sources of errors are also present but they can be easily controlled and made negligible (see, [18]). By increasing the number N of Monte Carlo steps the $1/\sqrt{N}$ -statistical error can be decreased as much as desired, at least in principle. In each application presented below, this error has been reduced to a level sufficient for our purposes. In contrast, the fixed-node approximation is much more challenging and its control is a crucial issue of present-day QMC approaches. It is known that the magnitude of the fixed-node error is directly related to the quality of the nodal structure of the approximate trial wavefunction used in the simulation [the nodes are the $(3N - 1)$ -dimensional zeroes of the $3N$ -dimensional wavefunction, N being the number of electrons]. Exact total energies can be obtained only when using trial wavefunctions having the nodes of the exact (unknown) wavefunction. It should be emphasized that, in contrast with the statistical error which can be reduced as desired by increasing Monte Carlo statistics, the fixed-node error is a *systematic error* (i.e., a bias) that survives even for infinite statistics. Numerical experience has shown that, although fixed-node energies are very accurate, non-negligible errors on energy differences may still occur due to improper cancellation of fixed-node errors. Unfortunately, in some cases this error can be large enough to lead to *qualitative* wrong conclusions. When considering closed-shell systems with a strong single-reference nature, nodal hypersurfaces resulting from single-determinant representations (*e.g.*, Hartree-Fock or Kohn-Sham type) are expected to be of sufficient quality. As we shall see, in the CuCl_2 case considered here, the situation is different. Although the exact wavefunction has a strong single-reference character, the presence of an open-shell makes the nodal structure of the wavefunction more difficult to describe. In this case the nodes of the $3N$ -dimensional wavefunction turn out to be very sensitive to the 3-dimensional nodal pattern chosen for the singly-occupied molecular orbital (SOMO). Note that it is an interesting case where the highly-complicated $3N$ -dimensional nodes usually so difficult to visualize can be reduced, in a good first approximation, to a much simpler 3D-pattern.

A last point to specify is the way spin-densities are computed here. In the case of total energies it is known that the only systematic error is the fixed-node one, despite the fact that the stationary diffusion Monte Carlo distribution is not exact. DMC actually samples the so-called mixed distribution given by the product of the trial wavefunction and the exact wavefunction, see [18]. In the case of properties other than energies, this is no longer true and some additional error related to the trial wavefunction contribution in the mixed distribution is present. This error can be removed in different (costly) ways, see *e.g.* [19] and [20]. However, such a possibility was not

considered here since, as we shall see later, the dominant source of error is the fixed-node approximation. Spin-densities are thus calculated in a standard way using a hybrid second-order estimate. For a general observable O it is expressed as[21]

$$\langle O \rangle \sim 2\langle O \rangle_{\text{DMC}} - \langle O \rangle_{\text{VMC}} \quad (2)$$

where averages are taken either over the mixed distribution sampled in DMC or over the squared trial wavefunction density sampled in a variational Monte Carlo (VMC) simulation. Here, the properties to be computed are the α and β spin densities and the quantities to average are merely the number of α or β electrons falling within histogram bins.

The all-electron Fixed-Node DMC spin-density for the ${}^2\Pi_g$ ground-state using a Hartree-Fock wavefunction as trial wavefunction (complemented with a standard Jastrow factor to reduce statistical fluctuations for the energy) is presented in Figure 5. The basis set used is that optimized in a previous work.[11] For comparison, the Hartree-Fock SD is also given. Although some differences between the two curves exist, they should essentially be considered as the same when compared to the typical differences present in the DFT-SD curves, Figure 2. The small differences include a slight increase of the main DMC peak and a small “spin-density wave” around Cl atoms. In this calculation the total energies obtained at the SCF and FN-DMC levels are -2558.1050 and -2560.719(2), respectively. To get an assessment of the accuracy reached here with QMC a rough estimate of the exact total energy of the molecule can be done. For that we add to the sum of atomic energies the atomization energy calculated at the SCF level. Taking for Cl the value from Davidson *et al.*,[22] for Cu the HF energy of Bunge,[23] plus the correlation energy estimate of Clementi *et al.*[24], the exact energy of separate atoms is found to be about -2560.868. Adding the SCF atomization energy we get a total ground-state energy for CuCl_2 of about -2561.045 a.u.. The percentage of correlation energy recovered by FN-DMC with HF nodes is thus quite large, roughly $\sim 89\%$. Thus, with this highly-correlated description of the wavefunction but imposing HF nodes, it is found that the shape of the SD is not quantitatively changed with respect to that obtained at the SCF level. Let us now consider the FN-DMC spin-densities obtained when using KS determinants instead of the Hartree-Fock one as trial wavefunctions. The KS determinants were obtained with standard B3LYP and with B3LYP with a variable amount of HF exchange. In Figure 6 the corresponding FN-DMC spin-densities are presented. As clearly seen, the overall shapes of FN-DMC spin-densities are tightly correlated with those obtained at the corresponding DFT level, see Figure 3. The results are thus similar to what has just been obtained for the SCF case: No qualitative change of the spin densities is obtained when passing from the variational to the FN-DMC level. These results strongly suggest that the key factor determining the SD shape is the nodal structure

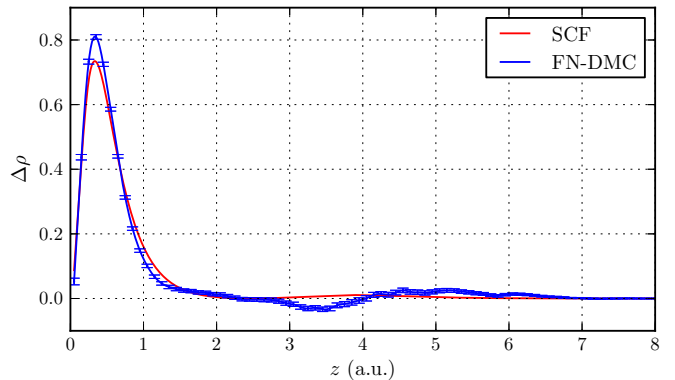


FIG. 5: ${}^2\Pi_g$ state spin density along the molecular axis (in a.u.) at the FN-DMC level with a HF trial wavefunction

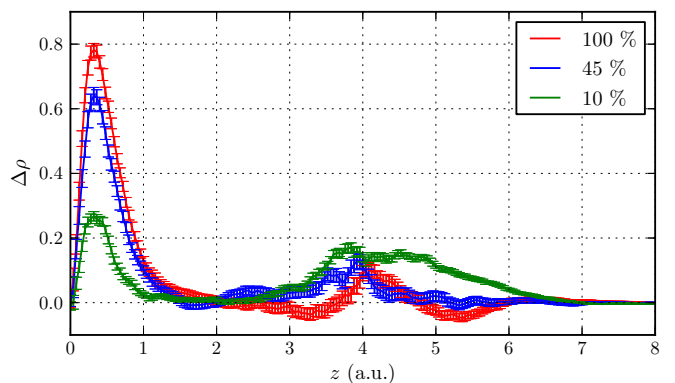


FIG. 6: ${}^2\Pi_g$ state FN-DMC spin densities along the molecular axis (in a.u.) using as trial wavefunction B3LYP-KS determinants obtained with different amounts of HF exchange

of the trial wavefunction used. The situation can thus be summarized as follows: i.) The amount of Hartree-Fock exchange in B3LYP determines the relative weight of $3p_{\text{Cl}}$ and $3d_{\text{Cu}}$ atomic contributions to the SOMO ii.) the nodes of the SOMO are directly related to this relative weight iii.) the nodal pattern of the whole trial wavefunction is dominated by the SOMO nodes. In the inset of Figure 2 a blow-up of the SOMO in the region around its node located at the middle of the Cu-Cl bond is presented; the two other nodes close to the secondary peak are weakly dependent on the level of exchange and will not be discussed here. The position of the central node is seen to be very sensitive to the percentage of HF exchange. Its location ranges from $R_{\text{node}} = 2.5$ for the Hartree-Fock wavefunction to about 2.05 for the KS determinant corresponding to the lowest HF percentage of 10%. In short, the nodes of the trial wavefunction are very sensitive and directly related the amount of HF exchange chosen. At this point, the situation is clearly not satisfactory since the overall shape of spin distributions is determined by the specific choice of nodes of the SOMO. Said differently, FN-DMC is not able to change qualitatively the global features of the spin-density associated with the approximate trial wavefunction given

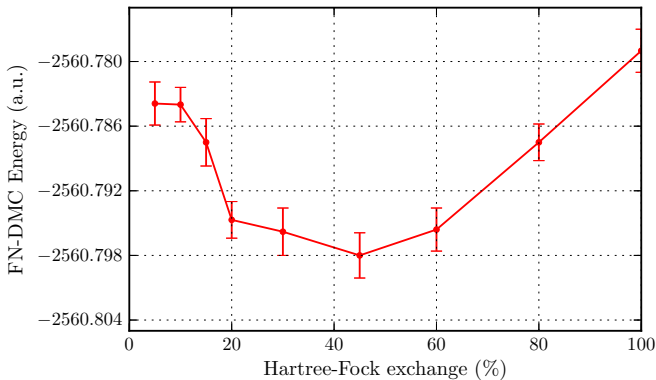


FIG. 7: Total FN-DMC ${}^2\Pi_g$ ground state energy obtained with a B3LYP determinant as a function of the HF exchange percentage for $CuCl_2$.

in input for the diffusion Monte Carlo process. We thus need to resort to alternative approaches capable of changing the nodes when electronic correlation effects are included. This will be the subject of the following section. Before that, let us nevertheless note that there exists in FN-DMC an internal criterion for estimating the nodal quality. It is based on the variational principle stating that the “better” the nodes are, the lower the fixed-node energies are expected to be.[21] Figure 7 presents the variation of the total FN-DMC ground-state energy as a function of the amount of exchange considered. The basis set employed in these calculations is that of Weigend and Ahlrichs,[25] which leads to significantly lower fixed-node energies than those obtained with the basis set proposed in Refs.[11] and [12]. Quite remarkably, a minimum is observed for a HF exchange percentage around 45%. This result is interesting and may be understood as a first indication of the typical amount of HF exchange that should be employed. However, let us stress that this result must be considered with lot of caution since the sensitivity of the FN-DMC results on nodal choice is high and optimizing only the one-dimensional nodes of the SOMO could be insufficient. Furthermore, optimizing nodes via minimization of the total energy is not a guarantee of improvement for other properties like spin density distributions.

VI. GROUND-STATE SPIN DENSITY WITH NEAR-FCI

In this section we report near-Full Configuration Interaction (FCI) calculations for total energies and spin-densities. To achieve converged results on this system including 63 electrons, a small 6-31G basis set is employed for both atoms, leading to a molecular basis of 51 orbitals. Although the accuracy reached with such a modest basis set can be questioned, it will allow us to investigate the major trends obtained when using multi-determinantal wavefunctions whose nodal structure may

change when correlation effects are introduced which, as we have shown, is not possible to do with FN-DMC. To realize FCI-type calculations for this system we use the CIPSI approach (Configuration Interaction with Perturbative Selection done Iteratively), a method proposed more than four decades ago (see, [26],[27], and more references in [28]) and very recently introduced in the context of QMC approaches.[28] For a detailed presentation of this approach the reader is referred to the original works. In short, CIPSI is a variational and multi-reference perturbational configuration interaction approach in which determinants that are to be included in the variational space are selected iteratively according to an energy criterion. Determinants perturbationally generated are added to the variational wavefunction when their perturbative contribution to the total energy is greater than a given threshold. In contrast with standard CI approaches where a whole set of particle-hole excitations are considered (single-excitations, single- and double-excitations, etc.), only excitations having a significant impact on the wavefunction expansion are selected as variational contributions. The relevance of a particular excitation is decided by comparing its energy contribution with the pre-fixed threshold. This procedure is applied iteratively until a given target number of determinants is reached. In practice, this leads to rather compact variational expansions consisting of a limited number of determinants in each type of excitations. Furthermore, higher-degree excitations not usually present in standard CI expansions may also be naturally introduced in the variational space with the CIPSI approach. Finally, let us note that several applications for a variety of metal-containing molecules have been realized during the 90’s, see *e.g.* [29],[30],[31]. The major difference between these applications and the present study is the size of the variational space that is taken much larger here (up to a million of determinants). The second-order perturbational correction is thus much reduced and an accuracy close to the FCI limit can be reached in the present application. In Figure 8 the convergence of the ground-state energy as a function of the number of determinants kept in the variational space is presented. To reduce the size of the variational CI calculation, molecular orbitals of the neon and argon cores for the chlorine and copper atoms, respectively, have been kept frozen. Calculations have been performed using 36 active molecular orbitals and 25 valence electrons. We stress that the size of the full CI space is about 10^{18} determinants. With the present basis set the maximum number of determinants in the variational space considered here is 10^6 . The three upper curves of Figure 8 are the variational energy curves corresponding to the multi-determinantal expansion, $|\Psi_0\rangle$ built using either SCF, DFT-B3LYP, or natural molecular orbitals. The latter were constructed from the variational CIPSI wavefunction obtained with 10^6 determinants. As seen on the figure, all curves are found to converge almost to the same value, as it should be when approaching the full CI limit. The lower curve

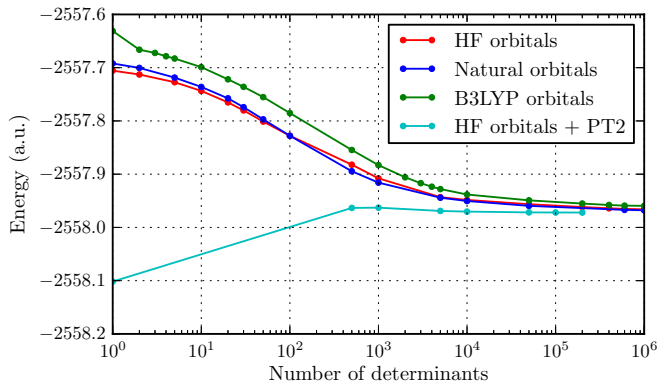


FIG. 8: Total variational (three upper curves) and variational + perturbational (lower curve) ground-state energy as a function of the number of determinants kept in the CIPSI selection process. SCF, B3LYP and natural orbitals are used.

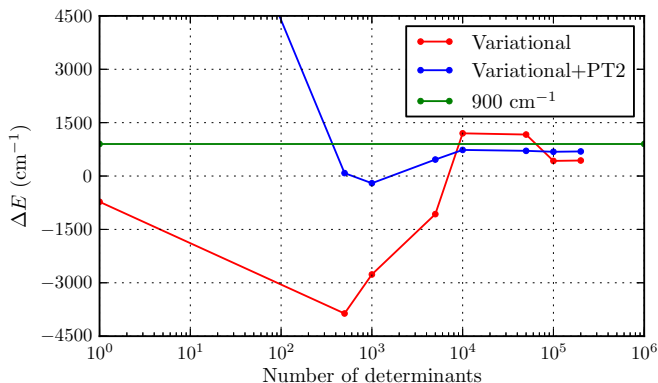


FIG. 9: ${}^2\Sigma_g - {}^2\Pi_g$ energy gap as function of the number of determinants in the variational space.

shows the so-called CIPSI energy obtained by adding to the variational energy E_0 the second-order perturbative contribution defined as

$$E_{PT2} = - \sum_{i \in P} \frac{\langle \Psi_0 | H | D_i \rangle^2}{\langle D_i | H | D_i \rangle - E_0}. \quad (3)$$

where P denotes the set of all determinants not present in the multi-determinantal expansion $|\Psi_0\rangle$ but connected to it by the Hamiltonian H (single- and double-excitations). For clarity only the CIPSI curve obtained with HF orbitals is shown, the other CIPSI curves have a similar behavior. E_{PT2} can be considered as a measure of the energy difference between the variational energy and FCI limit. As seen on the figure, the convergence of CIPSI energy is particularly rapid, we consider the limit has been attained with about 20 000-50 000 determinants in the variational space. For a large enough number of determinants, the perturbative correction E_{PT2} becomes quite small, this being a reliable indicator of the convergence to the FCI limit. In Figure 9 the energy difference between the ${}^2\Sigma_g$ and ${}^2\Pi_g$ states as a function of the number of determinants is presented (note the logarithmic scale for the

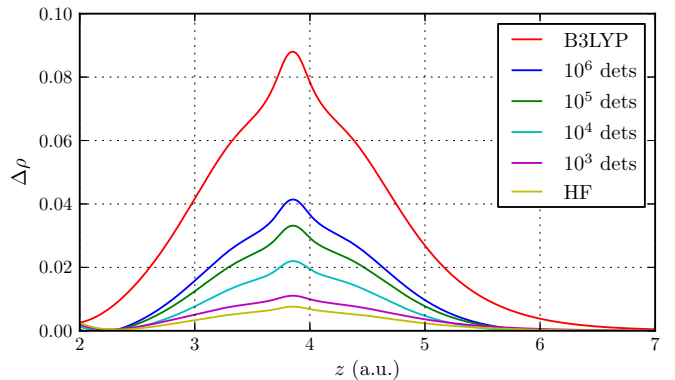


FIG. 10: ${}^2\Pi_g$ state. Spin density around the chlorine atom with HF, B3LYP and CIPSI with varying number of determinants. The basis set employed is 6-31G.

number of determinants). The evolution of the energy difference is shown both for the variational energies and the CIPSI energies (variational + E_{PT2}). At the purely variational level the ${}^2\Sigma_g - {}^2\Pi_g$ gap starts with a negative value (as it should be for one-determinant SCF wavefunctions, see Table I) and then changes sign when about 6 000 determinants are variationally included. With a larger number of determinants the energy gap is found to converge to a value close to about 1 000 cm^{-1} . At the CIPSI level, the convergence is even faster and better behaved. The CIPSI limit is close to the variational one. Note that for a small number of determinants the second-order energy correction is large and unphysical. CIPSI results are only meaningful in the large number of determinants regime, where the second-order contribution is indeed a correction.

Results obtained for the energy are very satisfactory; they demonstrate that nearly-FCI calculations are able to describe the transition between the two lowest electronic states despite the smallness of the basis set, since the converged value obtained for the energy gap is very close to the estimated SO-deperturbed value of about 900 cm^{-1} . For a deeper analysis we have also calculated the spin-density obtained from the CIPSI variational wavefunction. Its evolution as a function of the number of selected determinants is plotted in Figure 10. As usual, a two-peak structure is observed. In the figure only data for the secondary peak on the chlorine atoms are shown. For comparison, the SD obtained at the SCF (nearly vanishing small peak) and B3LYP levels (the highest peak) are also plotted. Remark that the maximum of the B3LYP peak is about 0.087, to compare with the value of 0.15 for the very same quantity presented in Figure 3 (ordinary B3LYP with 20% of HF exchange). We have checked that this difference results from basis set incompleteness due to the limitations of the 6-31G basis sets on both atoms. The CIPSI spin densities lie between both extreme curves and the height of the SD peak is found to increase continuously with the number of determinants in the variational space. For the maximum number of de-

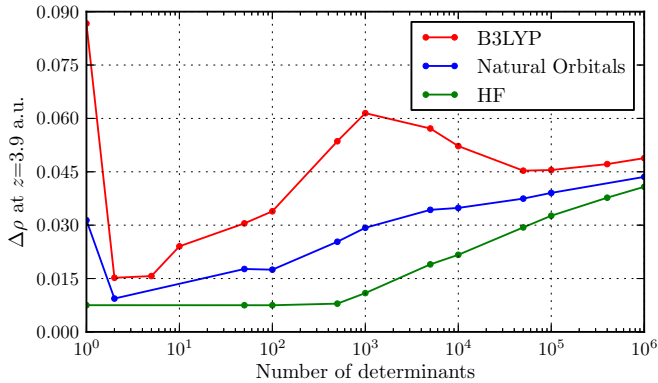


FIG. 11: ${}^2\Pi_g$ state. Convergence of the maximum of the secondary peak of the spin distribution as a function of the number of determinants in the variational space. Different types of molecular orbitals were used.

terminants of 10^6 the height of the peak is not yet fully converged but is large and represents about 40% of the B3LYP peak. In Figure 11 we present a more complete view of the convergence of the secondary peak as a function of the number of determinants selected, and with various types of molecular orbitals used in CIPSI. When using HF molecular orbitals, the spin density is found to remain close to zero up to a thousand of determinants and then begins to increase uniformly until it attains its maximum value. With B3LYP molecular orbitals the situation is qualitatively different. Starting from one determinant from a high value of the peak (as shown above with the B3LYP KS determinant), it decreases rapidly to a value close to zero. This phenomenon can easily be interpreted by noting that in a CI calculation the role of the first determinants consists essentially in lowering the energy via single-excitations whose effect is to optimize in an effective way the (natural) one-body orbitals (here, going from pure KS to SCF-type orbitals). Because of that, the SD is first found to almost vanish like in a SCF calculation. Next, when more determinants are added to the variational wavefunction, dynamical correlation contributions begin to enter the game (typically, through two-particle excitations) and then the SD starts to increase. Directly using natural orbitals, a similar phenomenon occurs but in a less marked way since the initial SD value is smaller than in the DFT case. To support the previous scenario regarding the role of single-excitations, we present in Figure 12 the shape of the secondary peak for a small number of determinants (about 50 determinants) using natural orbitals and including or excluding the SOMO-LUMO single-excitation that enters first in the variational space. Using only one determinant built with natural orbitals the maximum found for the peak is about 0.035, the largest value of the figure. Now, a short CIPSI calculation including only 50 determinants in the variational space is performed. Two situations are considered depending on the fact that the determinant representing the SOMO-LUMO single-excitation is

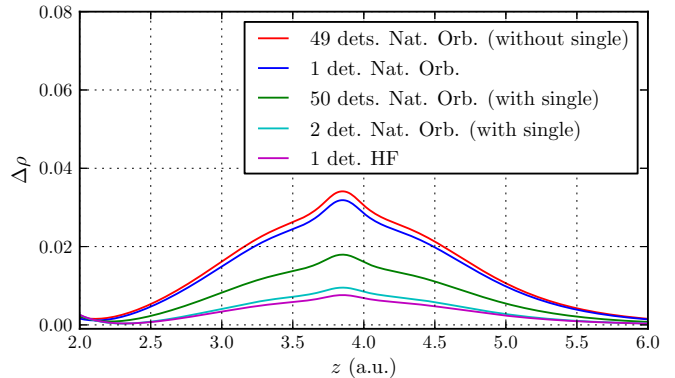


FIG. 12: Comparison of the secondary peak of the SD obtained with a small number of determinants, including or excluding the SOMO-LUMO single-excitation.

removed or not from the variational expansion. In the first case the peak is essentially unchanged. In sharp contrast, in the second case the peak of the spin distribution is significantly reduced and many additional determinants are needed to recover its original shape. These results nicely illustrate the role of single-excitations recovering the Hartree-Fock nature of the orbitals when a small number of determinants is considered in the reference space.

To conclude, results for the spin-density distribution along the molecular axis obtained using near-FCI calculations with the small 6-31G basis set lead to a particularly clear picture. At the SCF (or CASSCF) level, no spin density is present on the chlorine atoms. The Cu(3d) hole is strongly localized on the copper atom and the ground-state is of symmetry ${}^2\Sigma_g$ (i.e., a negative energy gap with our definition). However, when introducing dynamical electron correlation contributions via a nearly full-CI calculation, the situation changes dramatically. The ${}^2\Pi_g$ becomes the ground-state and the Cu(3d) hole is found to be partly delocalized over the chlorine atoms. Quantitatively, the SD peak located on the Cl atoms is roughly two times smaller than the peak obtained with standard B3LYP (with 20% HF exchange contribution) and is similar to that obtained using B3LYP but with a higher percentage of HF exchange of about 40% (see, Figure 3). A remarkable point is that this result appears to corroborate the fact that in FN-DMC optimal nodes were obtained with KS orbitals built using about the same percentage of HF exchange (see, Figure 7). Finally, we have made some attempts to extend these near-full CI calculations to larger basis sets (triple- ζ +polarization). Unfortunately, given the much larger size of the full-CI space, we were not able to reach a level of convergence sufficient to get reliable information.

VII. DISCUSSION AND SUMMARY

In this work calculations of the total energy and spin-density for the ${}^2\Pi_g$ ground state of the CuCl_2 molecule have been presented using various quantum-mechanical methods. Depending on the approach employed different qualitative and quantitative descriptions of the spatial distribution of the spin density along the molecular axis have been found. At the root of such discrepancies lie the different ways the electronic structure is described and approximated.

At the DFT level the description of the low-lying states of the molecule is very dependent on the type of exchange-correlation functional chosen. Recalling that hybrid functionals had been shown to provide the best agreement with experimental data, the energy gap between the two lowest states, ${}^2\Pi_g$ and ${}^2\Sigma_g$, is found to be very sensitive on the fraction of HF exchange used in the functional. For B3LYP the gap is roughly linearly dependent on this fraction, starting from a ${}^2\Sigma_g$ ground-state with 100% HF exchange to a ${}^2\Pi_g$ ground state with a sufficiently low percentage (about 40% and less). Regarding the spatial distribution of the spin density a similar strong dependence on the fraction of HF exchange used in the hybrid functional is found. In the case of the CuCl_2 molecule having a single unpaired electron, the DFT spin density is entirely determined by the square of the SOMO orbital. By varying the HF exchange percentage, the shape of this orbital may be continuously varied and so is the spin density. With the full HF exchange, the DFT spin-density is almost entirely localized on copper, while lower levels of HF exchange lead to increasingly delocalized spin densities on both Cl ligands. Such results are clearly disturbing, since there exists no internal criterion within DFT to decide which amount of HF exchange should be used and, thus, a meaningful chemical picture of the electronic distribution is difficult to obtain. We recall that in the DFT framework the self-interaction error (SIE) is known to be directly related to the exchange part of the functional; in the case of the metal-containing molecules with a high electronic density in the d shell this error may be particularly important and not easy to control, thus leading to a potentially incorrect description of the delocalization of electronic distributions.

A common way of shedding light on a situation where DFT leads to unpredictable results is to resort to highly-correlated post-Hartree-Fock methods where the construction of accurate $3N$ -dimensional wavefunctions allows, in principle, a better control of the details of the electronic structure but at a much higher computational price. At the HF level, and in agreement with hybrid DFT results with full HF exchange, the spin density is found to be completely localized on the central copper atom. At the CASSCF level including all $\text{Cl}(3p)$ and $\text{Cu}(3d,4s,4p)$ orbitals as active orbitals, the wavefunction is not significantly changed and is largely dominated by the HF determinant. In other words, the dynamical correlation effects are dominant here and the spin density

calculated with CASSCF is practically identical to that of the HF description. Unfortunately, as illustrated by a number of works, it is very difficult to reproduce with sufficient accuracy the dynamical correlation effects and thus to give a quantitative description of the low-lying states; in particular, to obtain the correct energy difference between the two lower states requires very high level calculations [*e.g.* CCSD(T) or ACPF] with large optimized basis sets. Unfortunately, these methods do not provide the final electronic density that would allow us to conclude on the true chemical picture concerning the spin density.

To escape from such limitations, we have proposed to resort to QMC calculations that are known to be particularly accurate. Using different types of trial wavefunctions fixed-node DMC calculations of both ground-state total energies and spatial distributions of the spin density have been performed. Unfortunately, although we get state-of-the-art total energies (we have estimated that about 90% of the total correlation energy for the ground-state energy is recovered), spin densities calculated within the fixed-node approximation are found to be too dependent on the nodal structure of the trial wavefunction employed. To be more precise, in the present case with a singly occupied molecular orbital (SOMO), we have seen that the complex $3N$ -dimensional nodal hypersurface of the full trial wavefunction is dominated by the 3-dimensional nodes of the SOMO and that the shape of the FN-DMC spin densities calculated is directly related to the shape of this orbital. Stated differently, qualitatively different spin density distributions can be obtained even at the supposedly very accurate FN-DMC level, depending on the choice of the singly-occupied orbital used in the trial wavefunction. Using a HF-type wavefunction, the FN-DMC spin density closely resembles to that obtained at the variational HF level. Similarly, when using various SOMO KS orbitals obtained with a variable exchange hybrid DFT method (here, B3LYP), FN-DMC spin densities resembling to their KS counterparts are obtained. As a consequence, it becomes impossible to decide on such grounds what is the correct chemical picture for the spin distribution. Nevertheless, we have noted that, within the framework of FN-DMC approaches, there exists an internal criterion allowing to estimate the nodal quality: The lower the fixed-node energy is, the “better” the nodes are expected to be (variational property of the fixed-node energy, see [21]). We have insisted on the fact that this criterion should be taken with lot of caution for a property other than the energy; however, it is worth noting that the nodes of the SOMO minimizing the fixed-node energy are those corresponding to a contribution of HF exchange of about 40-45%, considerably higher than the ordinary B3LYP but much smaller than pure HF.

In order to elucidate these various contradictory results and to get a plausible description of the ground-state spin-density distribution, we have proposed to perform near-full Configuration Interaction calculations. Only

such calculations can indeed yield a reliable balance between electron correlation and exchange effects. Obviously, in the present case where the molecule contains 63 electrons, ordinary FCI calculations using standard basis sets are just unfeasible. However, to circumvent this difficulty we have proposed to greatly reduce the dimensionality of the CI problem by employing the small 6-31G basis sets on both atoms and then by performing selected multireference CI calculations, which allowed us to avoid huge intractable multi-determinantal variational FCI expansions. Clearly, by using a small basis set the quantitative accuracy of the results can be questioned. However, since all types of electronic excitations are considered[32], it can be expected that chemically relevant trends regarding the various aspects obtained above with other methods may emerge. The multireference CI used here is a perturbatively selected CI scheme (CIPSI) that includes in a hierarchical way the most important determinants to asymptotically approach the FCI limit. Remarkably, it has been shown that using CIPSI for both the ground and first-excited state, these near-FCI calculations yield transition energies and spin-densities that are almost converged.

From the all set of data obtained for total energies, energy gap, spin densities, and the dependence of the various results on the number of determinants and types of molecular orbitals used, a rather coherent chemical picture emerges. At the uncorrelated (SCF) level, the lowest state is of ${}^2\Sigma_g^+$ symmetry and the Cu(3d) hole is completely localized on the copper atom. When dynamical correlation effects are added the ordering between the ${}^2\Sigma_g$ and ${}^2\Pi_g$ states is reversed and the hole is found

to partly delocalize over the Cl ligands. At the ordinary DFT-B3LYP level the Cu(3d) hole is too delocalized over the chlorine atoms due to an improper balance between the self-interaction and exchange effects. To get a chemically meaningful description of electronic distributions using B3LYP-DFT the percentage of HF exchange used must be increased up to about 40%. At the fixed-node DMC level, spin densities are found to be intimately related to the shape of the singly occupied molecular orbital, an orbital whose nodes are in turn directly related to the level of HF exchange used to derive it. Using as criterion the minimization of the FN-DMC ground-state energy, the optimal nodes for the SOMO are obtained for a HF exchange weight of about 40%, a result coherent with what has been obtained with near-FCI. Finally, let us note that the fact that DFT overestimates delocalization effects of magnetic holes in molecular systems has already been noticed in the literature by other authors (see, *e.g.* [33]).

Acknowledgments. We would like to acknowledge a fruitful discussion with Jeremy Harvey about the role of the exchange in metal-containing molecular systems. The Agence Nationale pour la Recherche (ANR) is thanked for support through Grant No ANR 2011 BS08 004 01. ARS thanks support from the 2013 CONACYT (Mexico) sabbatical program and from the Professeur Invité program from the Université de Toulouse (UPS). This work has been made possible through generous computational support from CALMIP (Toulouse) under the allocation 2012-0510, GENCI, and CCRT (CEA).

-
- [1] J.Tao, J.P. Perdew, V.Staroverov, G. Scuseria, Phys. Rev. Lett. 91, 146401 (2003).
- [2] A.D.Becke, Int. J. Quantum Chem. Symp. 28, 625 (1994).
- [3] J.P. Perdew, S. Kurth, A. Zupan and P. Blaha, Phys. Rev. Lett. 82, 2544 (1999); E.I. Proynov, A. Vela and D.R. Salahub, Chem. Phys. Lett. 230, 419 (1994).
- [4] A.D. Becke, J. Chem. Phys. 98, 1372. (1993).
- [5] J.P. Perdew J.Tao, V. Staroverov, G. Scuseria, C. Csonka, J. Chem. Phys. 123, 062201 (2005); J.P. Perdew, in A Primer in Density Functional Theory, Lecture Notes in Physics; edited by C. Fiolhais, F. Nogueira and M. Marques (Springer-Verlag, Berlin, 2003).
- [6] N.E. Schultz, Y. Zhao and D.G. Tryhlar, J. Phys. Chem. A 109, 4388 (2005).
- [7] F. Furche and J.P. Perdew, J. Chem. Phys. 124, 044103 (2006).
- [8] A. Ramírez-Solís, J. Chem. Phys. 126, 224105 (2007).
- [9] A.J. Ross, P. Crozet, R. Bacis, S. Churassy, B. Erba, S.H. Ashworth, N.M. Lakin, M.R. Wickham, I.R. Beattie and J.M. Brown, J. Mol. Spectrosc. 177, 134 (1996); A.J. Bouvier, E. Bosch and A. Bouvier, Chem. Phys. 202, 139 (1996); E. Bosch, P. Crozet, A.J. Roos and J.M. Brown, J. Mol. Spectrosc. 202, 253 (2000) and references therein.
- [10] M. Lorenz, N. Caspary, W. Foeller, J. Agreiter, A.M. Smith and V.E. Bondibey, Mol. Phys. 91, 483 (1997); M. Lorenz, A.M. Smith and V.E. Bondibey, J. Chem. Phys. 115, 8251 (2002).
- [11] A. Ramírez-Solís and J.P. Daudey, J. Chem. Phys. 120, 3221 (2004).
- [12] A. Ramírez-Solís and J.P. Daudey, J. Chem. Phys. 122, 14135 (2005).
- [13] C.W. Bauschlicher and B.O. Roos, J. Chem. Phys. 91, 4785 (1989).
- [14] A. Ramírez-Solís, R. Poteau, A. Vela and J.P. Daudey, J. Chem. Phys. 122, 164306 (2005).
- [15] F. Rogemond, H. Chermette and D.R. Salahub, Chem. Phys. Lett. 219, 228 (1994).
- [16] R.J. Deeth, J. Chem. Soc. Dalton Trans. 1061 (1993).
- [17] R. Assaraf, M. Caffarel, and A. Khelif, Phys. Rev. E 61, 4566 (2000).
- [18] M. Caffarel, Encyclopedia of Applied and Computational Mathematics, Ed. Bjorn Engquist, Springer, (2012).
- [19] M. Caffarel and P. Claverie, J. Chem. Phys. 88, 1088 (1988)
- [20] S. Baroni and S. Moroni, Phys. Rev. Lett. 82, 4745 (1999).
- [21] B.L. Hammond, W.A. Lester, Jr., and P.J. Reynolds in *Monte Carlo Methods in Ab Initio Quantum Chemistry*, World Scientific Lecture and course notes in chemistry Vol.1 (1994).

- [22] E.R. Davidson, S.A. Hagstrom, S.J. Chakravorty, V. Meiser Umar, and C. Froese Fischer, *Phys. Rev. A* **47**, 3649 (1993)
- [23] C.F. Bunge, J.A. Barrientos, A.V. Bunge, and J.A. Cogordan, *Phys. Rev. A* **46**, 3691 (1992)
- [24] E. Clementi and D.W.M. Hofmann, *J. Mol. Struct. (Theochem)* **330**, 17 (1995)
- [25] F. Weigend and R. Ahlrichs, *Phys. Chem. Chem. Phys.* **7**, 3297 (2005).
- [26] B. Huron, P. Rancurel, and J.P. Malrieu, *J. Chem. Phys.* **58**, 5745 (1973)
- [27] S. Evangelisti, J.P. Daudey, and J.P. Malrieu *Journal Chem. Phys.* **75**, 91 (1983).
- [28] E. Giner, A. Scemama, and M. Caffarel, *Can. J. Chem.* **91**, 879 (2013).
- [29] A. Ramírez-Solís and J.P. Daudey, *Chem. Phys.* **134**,111 (1989); A. Ramírez-Solís, J.P. Daudey, *J. Phys. B* **23**:2277 (1990); A. Ramírez-Solís and J.P. Daudey, *Phys. Rev. A* **42**, 5168 (1990); A. Ramírez Solís, J.P. Daudey, and C. Teichteil, *J. Chem. Phys.* **93**,7277(1990).
- [30] A. Ramírez-Solís and J. Schamps, *J. Chem. Phys.* **102**, 4482 (1995); A. Ramírez-Solís, J.P. Daudey, *J. Chem. Phys.* **113**, 8580 (2000).
- [31] A. Ramírez-Solís, M.E. Ruiz, O. Novaro, and J.P. Daudey J.P., *Z. Phys. D At. Mol. Clus.* **15**, 71 (1990).
- [32] In practice, excitations up to quintuples are treated variationally, those up to septuples perturbatively, the others having a negligible contributions.
- [33] J. Cabrero, C.J. Calzado, D. Maynau, R. Caballol, and J.P. Malrieu, *J. Phys.Chem. A* **106**, 8146 (2002).